Vascular Endothelial Growth Factor Contributes to Prostate Cancer–Mediated Osteoblastic Activity

Yasuhide Kitagawa,[1] Jinlu Dai,[1] Jian Zhang,[3] Jill M. Keller,[1] Jacques Nor,[2] Zhi Yao,[4] and Evan T. Keller[1]

[1]Department of Urology, School of Medicine, and [2]Department of Cariology, School of Dentistry, University of Michigan, Ann Arbor, Michigan; [3]Department of Internal Medicine, University of Pittsburgh, Pittsburgh, Pennsylvania; and [4]Department of Immunology, Tianjin Medical University, Tianjin, China

Abstract

Prostate cancer frequently metastasizes to bone resulting in the formation of osteoblastic metastases through unknown mechanisms. Vascular endothelial growth factor (VEGF) has been shown recently to promote osteoblast activity. Accordingly, we tested if VEGF contributes to the ability of prostate cancer to induce osteoblast activity. PC-3, LNCaP, and C4-2B prostate cancer cell lines expressed both VEGF-165 and VEGF-189 mRNA isoforms and VEGF protein. Prostate cancer cells expressed the mRNA for VEGF receptor (VEGFR) neuropilin-1 but not the VEGFRs Flt-1 or KDR. In contrast, mouse pre-osteoblastic cells (MC3T3-E1) expressed Flt-1 and neuropilin-1 mRNA but not KDR. PTK787, a VEGFR tyrosine kinase inhibitor, inhibited the proliferation of human microvascular endothelial cells but not prostate cancer proliferation *in vitro*. C4-2B conditioned medium induced osteoblast differentiation as measured by production of alkaline phosphatase and osteocalcin and mineralization of MC3T3-E1. PTK787 blocked the C4-2B conditioned medium–induced osteoblastic activity. VEGF directly induced alkaline phosphatase and osteocalcin but not mineralization of MC3T3-E1. These results suggest that VEGF induces initial differentiation of osteoblasts but requires other factors, present in C4-2B, to induce mineralization. To determine if VEGF influences the ability of prostate cancer to develop osteoblastic lesions, we injected C4-2B cells into the tibia of mice and, after the tumors grew for 6 weeks, administered PTK787 for 4 weeks. PTK787 decreased both intratibial tumor burden and C4-2B–induced osteoblastic activity as measured by bone mineral density and serum osteocalcin. These results show that VEGF contributes to prostate cancer–induced osteoblastic activity *in vivo*. (Cancer Res 2005; 65(23): 10921-9)

Introduction

Prostate cancer is the most frequently occurring cancer of males and second leading cause of cancer death in men in the United States (1). In metastatic prostate cancer, the primary site for metastasis is the skeleton, with 70% to 80% of prostate cancer patients developing skeleton metastases (2). Based on radiographic findings, bone metastases from prostate cancer have been described as osteosclerotic (i.e., having increased bone mineral formation). Histologically, they have been characterized with increased trabecular bone volume and newly woven bone (3), similar to that which develops in response to injury and is associated with accelerated osteoblastic activity (4). These structural changes in the metastatic lesions predispose the bone to fracture and are associated with severe pain. Thus, preventing progression of bone metastases may help improve the quality of life of prostate cancer patients. Accordingly, understanding the mechanisms that promote prostate cancer–induced osteosclerosis may help identify targets to diminish the progression of these lesions.

Prostate cancer cells produce a variety of factors that have direct or indirect osteogenic properties (5–7). Some of these factors, such as bone morphogenetic proteins (BMP) and endothelin-1, may directly stimulate differentiation of osteoblast precursors to mature mineral-producing osteoblasts (8–11). Other factors, such as parathyroid hormone-releasing protein, may work through inhibition of osteoblast apoptosis (12, 13). Cellular and molecular cross-talk between prostate cancer cells and the osteoblasts through these soluble factors can play important roles resulting in abnormal bone function; however, these factors have not been shown to induce osteoblast activity in the context of prostate cancer *in vivo*.

Vascular endothelial growth factor (VEGF) is a key regulator of physiologic and pathophysiologic angiogenesis (14). VEGF promotes endothelial cell proliferation, survival, and migration. The biological effects of VEGF are mediated by several receptors (15–17). Two receptor tyrosine kinases [VEGF receptor (VEGFR)-1 (also known as Flt-1) and VEGFR-1 (also known as KDR or Flk-1)] are the key VEGFRs. Additionally, a nonsignaling protein that binds collapsin-semaphorin family members (neuropilin-1) is a VEGFR. In addition to its effect on endothelial cells, VEGF stimulates migration of primary human osteoblasts (18) and osteoblast differentiation (19, 20). Furthermore, we showed previously that BMPs contribute to prostate cancer–mediated osteoblastic activity *in vitro* partly through VEGF (21). These data, together with reports that prostate cancer cells express VEGF *in vitro* and *in vivo* (22), led us to hypothesize that VEGF contributes to osteoblastic lesion formation at prostate cancer bone metastatic sites *in vivo*.

In the present study, we used PTK787, a tyrosine kinase inhibitor designed to inhibit VEGF signal transduction by binding directly to the ATP-binding sites of VEGFRs (23), to evaluate the role of VEGF in prostate cancer–mediated induction of osteoblastic activity *in vitro* and *in vivo*.

Materials and Methods

Cell culture. The human prostate cancer cell lines PC-3 and LNCaP were obtained from American Type Tissue Collection (Rockville, MD) and maintained in RPMI 1640 containing 10% fetal bovine serum (FBS), 100 units/mL penicillin, and 100 μg/mL streptomycin. C4-2B cells, which are LNCaP sublines, were obtained from UroCor, Inc. (Oklahoma City, OK)

Requests for reprints: Evan T. Keller, Room 5304 CCGCB Box 0940, 1500 East Medical Center Drive, Ann Arbor, MI 48109-0940. Phone: 734-615-0280; Fax: 734-936-9220; E-mail: etkeller@umich.edu.

doi:10.1158/0008-5472.CAN-05-1809

Table 1. PCR primers used to evaluate VEGF and VEGFR mRNA expression

Primer	Forward	Reverse	Amplicon size (bp)
VEGF-165	5′-CGGATCAAACCTCACCAAGGCC-3′	5′-CTTTCTCCGCTCTGAGCAAGGC-3′	132
VEGF-189	5′-CGGATCAAACCTCACCAAGGCC-3′	5′-CTTTCTCCGCTCTGAGCAAGGC-3′	204
Human Flt-1	5′-GCACCTTGGTTGTGGCTGAC-3′	5′-CGTGCTGCTTCCTGGTCC-3′	585
Human KDR	5′-GTCAAGGGAAAGACTACGTTGG-3′	5′-AGCAGTCCAGCATGGTCTG-3′	591
Human neuropilin-1	5′-AGGACAGAGACTGCAAGTATGAC-3′	5′-AACATTCAGGACCTCTCTTGA-3′	209
Mouse Flt-1	5′-GGCTCAGGGTCGAAGTTAAAAGTGCCT-3′	5′-CATGTAGGCCATGAGGTCCACCAC-3′	625
Mouse KDR	5′-CTCTGTGGGTTTGCCTGGCGATTTTCT-3′	5′-GCGGATCACCACAGTTTTGTTCTTGTT-3	408
Mouse neuropilin-1	5′-GGCTGCCGTTGCTGTGCG-3′	5′-ATAGCGGATGGAAAACCC-3′	404
Human GAPDH	5′-TGAAGGTCGGTGTGAACGGATTTGGT-3′	5′-CATGTAGGCCATGAGGTCCACCAC-3′	289

and maintained in T medium containing 10% FBS, 100 units/mL penicillin, and 100 μg/mL streptomycin as outlined by UroCor. MC3T3-E1 cells are pre-osteoblasts derived from murine calvarias that, when treated with ascorbate, express osteoblast-specific markers and are capable of producing a mineralized matrix (24, 25). These cells (a kind gift from Dr. Renny Franceschi, University of Michigan, Ann Arbor, MI) were routinely maintained in α-MEM containing 10% FBS, 100 units/mL penicillin, and 100 μg/mL streptomycin. Human dermal microvascular endothelial cells (HDMEC) were obtained from Clonetics (San Diego, CA), grown in EBM-2 basal medium plus EGM-2MV Bullet kit (Clonetics), and used between passages 4 and 7 for experiments. Human bone marrow endothelial cells (HBMEC) were obtained from American Type Tissue Collection and maintained in DMEM containing 10% FBS, 100 units/mL penicillin, and 100 μg/mL streptomycin.

Primary osteoblastic cells were derived from human cancellous bone explants obtained as waste tissue from hip replacement surgeries as described previously (26, 27). Briefly, specimens were collected from human subjects undergoing hip replacement. Trabecular bone chips were washed extensively in PBS to remove bone marrow and then treated by sequential digestion with collagenase P (Boehringer Mannheim, Indianapolis, IN). Collagenase-released cells were plated and cultured in DMEM containing 10% FBS, 100 units/mL penicillin, and 100 μg/mL streptomycin. These cells expressed the phenotype of mature osteoblastic cells. This protocol was approved by the University of Michigan Human Subjects Internal Review Board.

Conditioned medium. Cancer cells were grown to 80% to 90% confluence in their respective medium containing 10% FBS in T-75 flask. The medium was removed and the cells were washed with PBS. Cells were incubated for 24 hours in 15 mL serum-free medium. After 24 hours, conditioned medium was collected, concentrated with Biomax centrifugal filter device (molecular weight cutoff 10 kDa; Millipore Corp., Bedford, MA), and then frozen. Before use, protein concentration was determined by the Lowry method (BCA Protein Assay Reagent kit, Pierce Biotechnology, Inc., Rockford, IL).

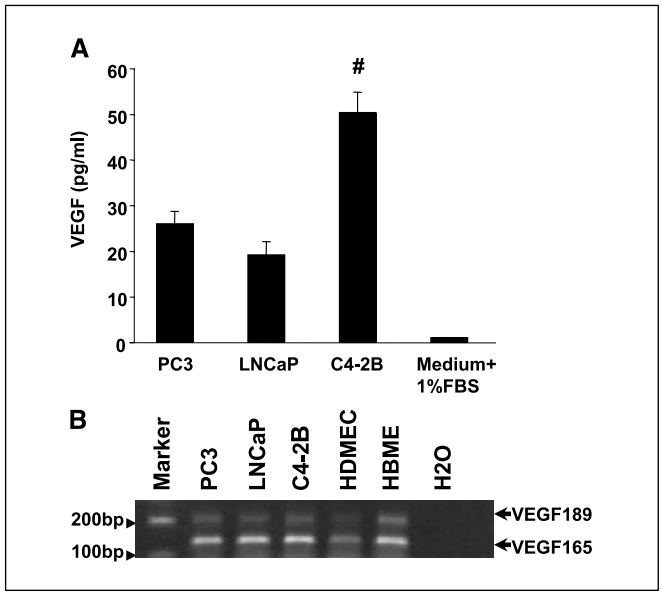

Figure 1. Prostate cancer cells express VEGF. Human prostate cancer cells (1×10^5 per well) were plated in 12-well plates in medium plus 10% FBS. They were incubated overnight and changed to medium plus 1% FBS. After 48 hours, cell culture supernatants were collected, cells were counted, and total RNA was collected. *A,* culture supernatants were subjected to VEGF ELISA. Results were normalized to final cell number (per 10^4). *Columns,* mean; *bars,* SD. #, $P < 0.05$ versus PC-3 and LNCaP (ANOVA and Fisher's protected least significant difference for post hoc analysis). *B,* RT-PCR was done on 1 μg total RNA extracted from prostate cancer cells and HDMECs or HBMECs. Markers (100 bp) were used in these studies.

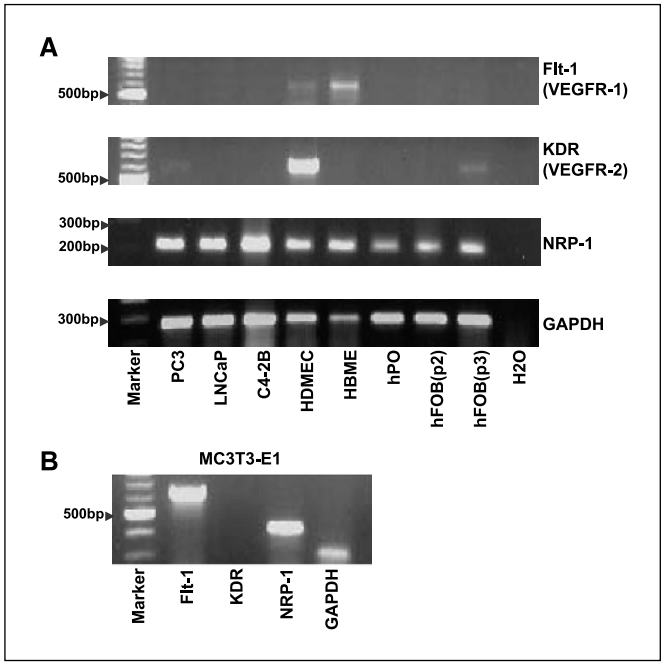

Figure 2. Expression of VEGFRs in prostate cancer cells, osteoblasts, and endothelial cells. *A,* RT-PCR using PCR primers for the indicated human VEGFRs was done on 1 μg total RNA from the indicated prostate cancer cell lines and HDMECs, HBMECs, human primary osteoblasts (*hPO*), and second passage [*hFOB(p2)*] or third passage [*hFOB(p3)*] human fetal osteoblasts. *B,* RT-PCR using PCR primers for the indicated murine VEGFRs was done on 1 μg total RNA from the murine pre-osteoblast MC3T3-E1 cells. Markers (100 bp) were used in these studies. The size of at least one band on the marker is indicated for size reference.

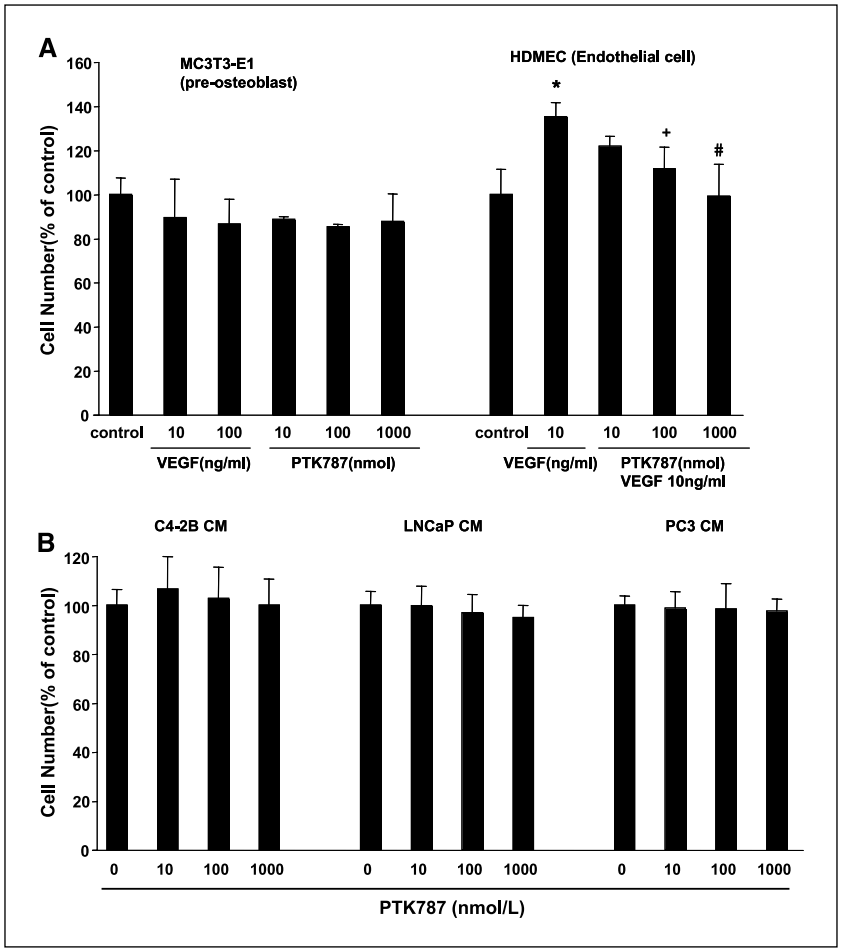

Figure 3. PTK787 inhibits the proliferation of HDMEC but not MC3T3-E1 and human prostate cancer cells. Cells (5×10^4 per well) were plated in 12-well plates in medium plus 10% FBS and incubated overnight. *A,* MC3T3-E1 was changed to α-MEM plus 2% FBS and indicated concentrations of PTK787 or rhVEGF-165. HDMEC was changed to EBM-2 basal medium plus 2% FBS, 10 ng/mL rhVEGF-165, and various concentrations of PTK787. *B,* prostate cancer cells were changed to RPMI 1640 plus 2% FBS and indicated concentrations of PTK787. After 72 hours, cells were trypsinized and cells were counted using trypan blue staining. *Columns,* mean; *bars,* SD. *, $P < 0.01$ versus control; +, $P < 0.05$; #, $P < 0.01$ versus 10 ng/mL VEGF without PTK787 (ANOVA and Fisher's protected least significant difference for post hoc analysis).

Reagents. VEGF-165 recombinant protein was obtained from R&D Systems (Minneapolis, MN). PTK787, a VEGFR tyrosine kinase inhibitor, was synthesized in the Department of Oncology Research, Novartis Pharmaceuticals (Basel, Switzerland). For *in vitro* assays, a stock solution of 10 mmol/L PTK787 was prepared in DMSO. This was diluted further in buffer or medium so that the concentration of DMSO in assay systems did not exceed 0.1%.

Assays for specific proteins. VEGF protein concentration was measured using a commercially available ELISA (R&D Systems). The sensitivity of this assay is 5.0 pg/mL. For measurement of alkaline phosphatase and mouse osteocalcin, MC3T3-E1 cells were plated in 12-well tissue culture plates at a density of 5×10^4 and grown in α-MEM containing 10% FBS. When cells were fully confluent, designated as day 0, the medium was removed and replaced with conditioned medium that contained 100 μg/mL protein levels. Additionally, 10% FBS, 50 μg/mL ascorbic acid (Sigma Chemical Co., St. Louis, MO), 10 mmol/L β-glycerophosphate (Sigma), and various concentrations of PTK787 were added. Medium was changed every 3 days. At days 9 and 15, conditioned medium was collected. The conditioned medium from day 9 was used to measure alkaline phosphatase activity, which was measured in supernatants using a colorimetric assay based on the conversion of *p*-nitrophenylphosphate as directed by the manufacturer (alkaline phosphatase assay; Sigma). Mouse osteocalcin was measured in culture supernatants and serum using a mouse osteocalcin enzyme immunoassay (Biomedical Technology, Inc., Stoughton, MA) as directed by the manufacturer. The sensitivity of this assay is 1.0 ng/mL. Serum total prostate-specific antigen (PSA) levels were determined using the Accucyte Human PSA Assay (Cytimmune Sciences, Inc., College Park, MA). The sensitivity of this assay is 0.488 ng/mL.

Measurement of mineralization. To stain mineral, cultures were either fixed in 95% ethanol at 37°C for 5 minutes, rehydrated, and then stained using the von Kossa method as described previously (27) or stained for alizarin red as described previously (27). Briefly, the medium was removed and the cells were air dried, fixed in 50% ethanol thrice, and then stained with alizarin red (Sigma; 100 mg/mL in 0.01% NaOH) for 5 minutes. After a PBS wash, retained dye was extracted in a solution of 20% methanol and 10% acetic acid, and the absorbance was measured at $A_{450\ nm}$.

Reverse transcription-PCR. VEGF and VEGFR mRNA levels were determined using reverse transcription-PCR (RT-PCR). The total RNA was purified using TRIzol (Life Technologies, Inc., Carlsbad, CA). Total RNA (1 μg) was reverse transcribed and amplified using Access RT-PCR system (Promega, Madison, WI) according to the manufacturer's protocol. PCR for human VEGF, Flt-1 (VEGFR-1), KDR (VEGFR-2), neuropilin-1, and glyceraldehyde-3-phosphate dehydrogenase (GAPDH) were done using primer sets indicated in Table 1. Thirty-five cycles of PCR were done with 1-minute denaturation at 94°C, 1-minute annealing at 55°C, 1-minute extension at 72°C, and final 7-minute extra extension at the end of the reaction to ensure that all amplicons were completely extended.

Animal studies. Male 8-week-old Fox Chase severe combined immunodeficient (SCID) mice (Charles River, Wilmington, MA) were injected intratibially with C4-2B cells (10^5 in 25 μL RPMI 1640) as described previously (28). The tumors were allowed to grow for 6 weeks, and mice were randomized into two groups as follows: group 1 ($n = 10$) oral administration of 100 mg/kg PTK787 daily and group 2 ($n = 13$) oral administration of distilled water (vehicle). For *in vivo* administration, PTK787 was dissolved in DMSO to a concentration of 100 mg/mL and then diluted with distilled water to a final concentration of 5 mg/mL. The PTK787 was given by once daily oral gavage of 0.50 mL of the 5 mg/mL solution to give a dose of 100 mg/kg. The PTK787 gavage solution was made fresh weekly. After 4 weeks of treatment, blood samples and radiographs were taken under anesthesia, and tibiae were harvested. In a parallel

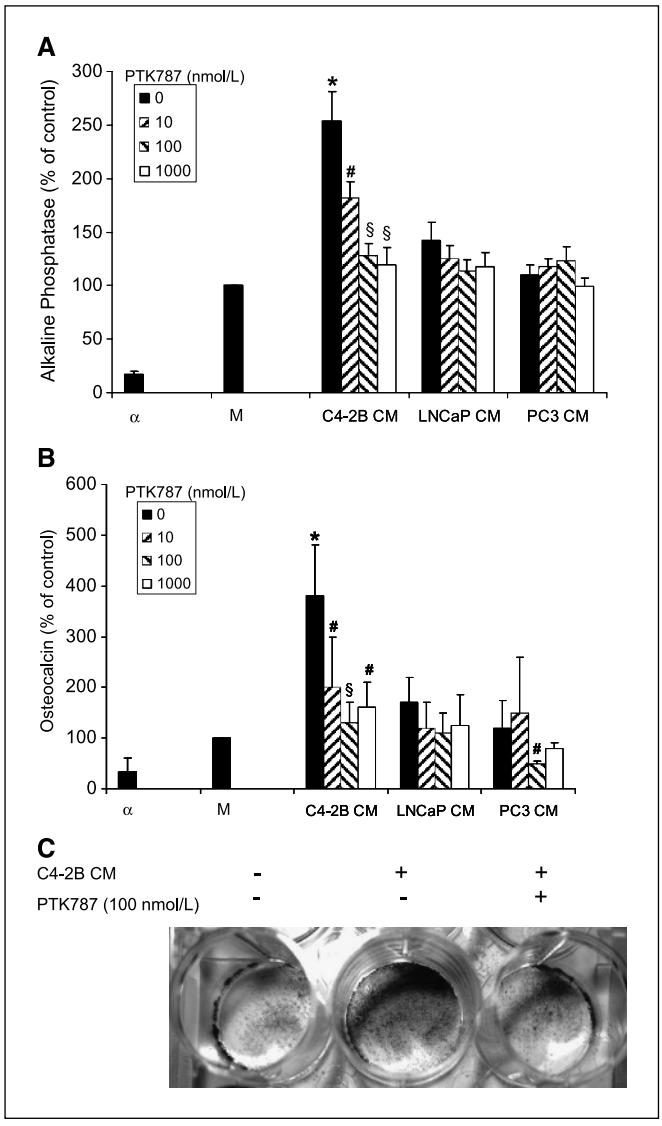

Figure 4. C4-2B conditioned medium induces osteoblast differentiation that is diminished by PTK787. MC3T3-E1 cells (5×10^4 per well) were plated in 12-well plates and grown in α-MEM containing 10% FBS. After the cells were confluent, the medium was removed and replaced with conditioned medium concentrated to a protein concentration of 100 μg/mL and the addition of 10% FBS, 50 μg/mL ascorbic acid, 10 mmol/L β-glycerophosphate, and the indicated concentrations of PTK787. Medium was changed every 3 days. In some wells, at days 9 and 15, conditioned medium was collected. Alkaline phosphatase (*A*) and osteocalcin (*B*) were measured in supernatants of days 9 and 15 conditioned medium, respectively. After medium was removed at day 15, wells were stained using the von Kossa method to detect mineralization (*C*) which is detected as gray. Control for mineralization medium (*M*) consisted of α-MEM, including 10% FBS, 50 μg/mL ascorbic acid, and 10 mmol/L β-glycerophosphate. α-MEM plus 10% FBS was used as negative control (α). Results were normalized to mineralization medium as 100%. *Columns,* mean of three experiments; *bars,* SD. *, $P < 0.05$ versus negative control; §, $P < 0.05$ versus control; #, $P < 0.05$ versus 0 nmol/L PTK787 in C4-2B conditioned medium (ANOVA and Fisher's protected least significant difference for post hoc analysis).

protocol to determine the effects of PTK787 on normal bone remodeling, mice without tumor injection were treated with vehicle or PTK787 daily for 4 weeks. Then, serum and tibia were collected. These animal protocols were approved by the University of Michigan Animal Care and Use Committee.

Dual-energy X-ray absorptiometry measurement and X-ray. Bone mineral density (BMD) of the excised tibiae were measured using dual-energy X-ray absorptiometry (DEXA) on an Eclipse peripheral DEXA Scanner using pDEXA Sabre software version 3.9.4 in research mode (Norland Medical Systems, Fort Atkinson, WI). Bones were scanned at 2 mm/s with a resolution of 0.1 × 0.1 mm. Three 0.5-cm regions of interest were randomly selected for each fragment to determine BMD. Short-term BMD precision (% coefficient of variation) was ~3% for this technique. Radiographs were taken after excision of bone implants by using a Faxitron (Faxitron X-ray Corp., Wheeling, IL).

Bone histopathology. Histopathology was done as we have described previously (28). Briefly, bone specimens were fixed in 10% formalin for 24 hours and then decalcified using 12% EDTA for 72 hours. The specimens were then paraffin embedded, sectioned (5 μmol/L), and stained with H&E to assess histology. Midsagittal sections were used to quantify tumor area, which was measured as the percentage of tumor present in the total area of nonmineralized bone tissue as described previously (29).

Data analysis. Statistical significance was determined for multivariate comparisons using ANOVA and Fisher's protected least significant difference for post hoc analysis. Student's *t* test was used for bivariate analyses. Statistical significance was determined as $P < 0.05$. Statistical calculations were done using Statview software (Abacus Concepts, Berkeley, CA).

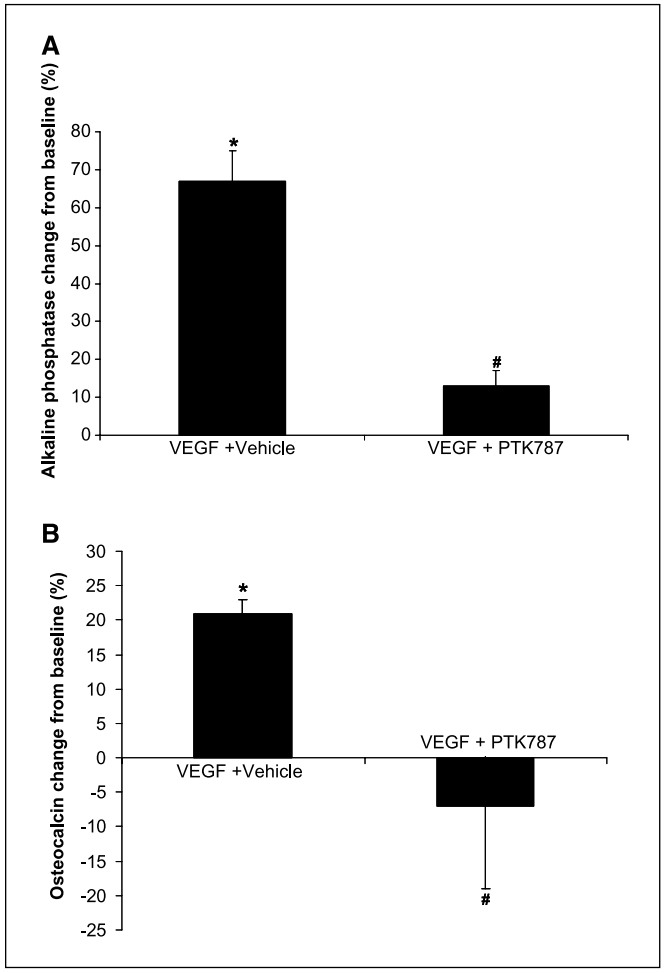

Figure 5. VEGF directly induces alkaline phosphatase and osteocalcin levels in MC3T3-E1 cells. MC3T3-E1 cells were plated (5×10^4 per well) in 12-well plates and grown in α-MEM containing 10% FBS. After the cells were confluent, the medium was replaced with α-MEM, including 10% FBS, 50 μg/mL ascorbic acid, 10 mmol/L β-glycerophosphate, and 50 nmol/L PTK787 and/or 100 ng/mL rhVEGF-165. Medium was changed every 3 days. At days 9 and 15, conditioned medium was collected and alkaline phosphatase (*A*) and mouse osteocalcin (*B*) were measured, respectively. Levels measured in medium alone were set as baseline. *Columns,* mean percent change from baseline from three separate experiments; *bars,* SD. *, $P < 0.05$ versus baseline (i.e., no VEGF); #, $P < 0.05$ versus VEGF + Vehicle (ANOVA and Fisher's protected least significant difference for post hoc analysis).

Results

To detect and quantify VEGF production in prostate cancer cells, PC-3, LNCaP, and C4-2B prostate cancer cells were grown in culture and the conditioned medium was collected and subjected to ELISA. All three cell lines expressed VEGF protein; however, it was 2-fold higher in the supernatant from C4-2B compared with that from the LNCaP and PC-3 cells (Fig. 1*A*). To further identify which isoforms of VEGF were expressed in the prostate cancer cell lines, total RNA was collected and subjected to PCR analysis. The PCR product size for VEGF-165 and VEGF-189 were 132 and 204 bp, respectively. All three prostate cancer cell lines expressed both VEGF-165 and VEGF-189 mRNA isoforms (Fig. 1*B*). Endothelial cells also expressed VEGF mRNA (Fig. 1*B*). These findings show that VEGF protein and mRNA are present in prostate cancer cell lines.

To detect if prostate cancer cells express the receptors for VEGF, we subjected total RNA to PCR for VEGFRs. The PCR product size for human Flt-1 and KDR was 585 and 591 bp, respectively. Prostate cancer and human osteoblast cells had no or very little expression of Flt-1 and KDR mRNA (Fig. 2*A*). HDMEC expressed high levels of KDR and Flt-1 mRNA. HBME expressed Flt-1 but not KDR. Neuropilin-1 mRNA, for which the PCR product size was 209 bp, was expressed in all cell lines we used (Fig. 2*A*). The PCR product size for mouse Flt-1, KDR, and neuropilin-1 was 625, 408, and 404 bp, respectively. Murine MC3T3-E1 cells expressed Flt-1 and neuropilin-1 mRNA but not KDR (Fig. 2*B*).

VEGF has proliferative effects on several cell types. It is possible that VEGF may modulate the development of bone metastases through increasing proliferation of cell types present in the bone metastatic sites, such as prostate cancer cells, osteoblasts, and endothelial cells. To determine if VEGF directly modulated proliferation of cells found in the bone metastasis microenvironment, we examined the effect of VEGF on the proliferation of prostate cancer cells, an osteoblast cell line, MC3T3-E1, and an endothelial cell line, HDMEC, *in vitro*. Neither recombinant human VEGF (rhVEGF)-165 nor PTK787 affected MC3T3-E1 proliferation (Fig. 3*A*). In contrast, rhVEGF-165 stimulated HDMEC proliferation, and 100 nmol/L PTK787 partially inhibited rhVEGF-induced proliferation of HDMEC and 1,000 nmol/L PTK787 completely inhibited rhVEGF-induced proliferation (Fig. 3*A*). Finally, neither VEGF nor PTK787 affected prostate cancer cell proliferation (Fig. 3*B*; data not shown). These results suggest that VEGF induces proliferative effects on endothelial cells but not osteoblasts or prostate cancer cells.

Prostate cancer cells promote osteoblastic activity, including alkaline phosphatase production and osteocalcin production and mineralization, in pre-osteoblastic cells (17, 21). Furthermore, it has been reported that VEGF induces osteoblastic activity (30). Based on these findings, we examined if VEGF contributes to the ability of prostate cancer cells to promote osteoblastic activity. Accordingly, we added C4-2B conditioned medium to MC3T3-E1 cells and measured alkaline phosphatase (an indicator of early osteoblast differentiation) and osteocalcin (a measure of late osteoblast differentiation) levels. C4-2B conditioned medium induced MC3T3-E1 cells to produce both alkaline phosphatase and osteocalcin (Fig. 4*A* and *B*; compare C4-2B conditioned medium versus mineralization medium alone). PTK787 diminished C4-2B-induced alkaline phosphatase and osteocalcin expression in MC3T3-E1 cells (Fig. 4*A* and *B*). LNCaP and PC-3 conditioned medium did not induce osteocalcin expression (Fig. 4*A* and *B*). To further identify the ability of the dependency of C4-2B on VEGF to induce osteoblastic activity, we assessed *in vitro*

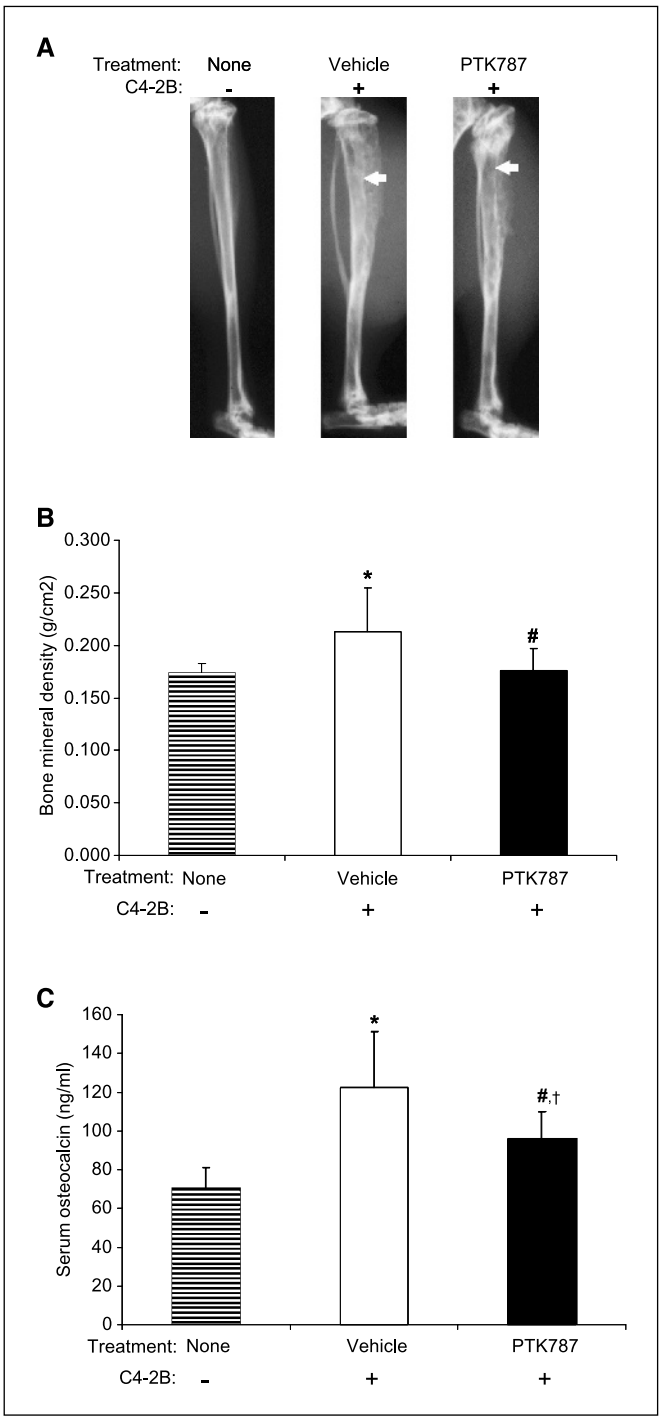

Figure 6. VEGF contributes to C4-2B-mediated increased osteoblastic activity *in vivo*. SCID mice were injected intratibially with C4-2B cells (10^5 in 25 μL RPMI 1640). After 6 weeks of tumor growth, treatment with either PTK787 ($n = 12$) or distilled water vehicle ($n = 9$) was initiated and continued for 4 weeks at which time mice were euthanized, bones were subjected to Faxitron X-ray analysis and DEXA, and blood was collected and separated into serum that was subjected to enzyme immunoassay for osteocalcin. *A,* radiographs taken on Faxitron. Note the increased opacity in the marrow cavity (*arrow*) in the tibia of the vehicle-treated mouse compared with normal tibia without tumor (*None*). In contrast, the PTK787-treated animals have less opacity (*arrow*) than the tibiae for the vehicle-treated or normal mice. *B,* BMD measured by DEXA. *, $P < 0.03$ versus normal animal (i.e., no treatment and no C4-2B cancer cells); #, $P < 0.03$ versus vehicle-treated animals (ANOVA and Fisher's protected least significant difference for post hoc analysis). *C,* serum osteocalcin levels. *, $P < 0.01$ versus normal animal; #, $P < 0.02$ versus vehicle-treated animals; †, $P < 0.04$ versus normal animal (ANOVA and Fisher's protected least significant difference for post hoc analysis).

mineralization. C4-2B conditioned medium induced *in vitro* mineralization and that was diminished by PTK787 (Fig. 4*C*). These results show that C4-2B cells induce osteocalcin, at least in part, through VEGF.

The *in vitro* studies indicated that VEGF contributes to prostate cancer–induced bone remodeling; however, they do not show if VEGF does this directly through modulation of osteoblasts or indirectly through acting on some intermediate cells. To determine if VEGF directly induces osteoblastic activity, we added VEGF into MC3T3-E1 cell cultures and measured alkaline phosphatase, osteocalcin, and mineralization. VEGF induced both alkaline phosphatase and osteocalcin expression and this was diminished by PTK787 (Fig. 5). In contrast, VEGF did not induce mineralization (not shown). PTK787 (50 nmol/L) alone had no effect on alkaline phosphatase or osteocalcin expression or mineralization (data not shown). These results show that VEGF can induce early and late osteoblast differentiation markers but requires other factors produced by the prostate cancer cells to induce mineralization of MC3T3-E1 cells.

To determine if VEGF plays a role in the ability of prostate cancer cells to form osteoblastic lesions *in vivo*, we injected C4-2B cells into the tibiae of mice. Tumors were allowed to become established over a 6-week period, and administration of PTK787 or vehicle (5% DMSO and distilled water) was initiated and continued for 4 weeks at which time animals were euthanized. In the PTK787 group, 9 of 10 animals developed intratibial tumors; similarly, in the vehicle group, 12 of 13 animals developed tumors. The animals that did not develop tumors were excluded from the analyses. C4-2B tumors produced mixed osteoblastic/osteolytic lesions with an overall increase in BMD compared with normal tibiae (Fig. 6*A* and *B*). PTK787 diminished the C4-2B-induced increased of BMD. Consistent with the increase in BMD, serum osteocalcin levels were increased in mice with C4-2B tumors compared with mice without tumors (Fig. 6*C*). PTK787 diminished the C4-2B-induced increase of serum osteocalcin levels but not to the levels of mice without tumors. Histologic analysis revealed that C4-2B induced new bone formation (Fig. 7). Islands of tumor cells were surrounded by disorganized new bone. Consistent with the BMD data, PTK787 diminished the C4-2B-induced bone production (Fig. 7). In the vehicle-treated mice, the intratibal bone marrow was replaced by tumor cells. In contrast, PTK787 diminished the intratibial tumor area by ~15% (Fig. 8*A*). In correlation with the decreased tumor area, PSA levels were decreased in the PTK787-treated group compared with the vehicle-treated group (Fig. 8*B*).

Our results indicated that VEGF contributes to prostate cancer–induced bone remodeling, which is pathophysiologic bone remodeling. To determine if altering VEGF modulates the quality of healthy normally remodeling bone, we evaluated the BMD and serum osteocalcin levels in a set of normal mice that were treated with PTK787 for 4 weeks similar to the tumor-injected animals. Neither BMD (Fig. 9*A*) nor serum osteocalcin (Fig. 9*B*) levels differed among the vehicle or PTK787 treatment groups. This suggests that VEGF does not play a significant role in nonpathologic bone remodeling in a 4-week period as opposed to tumor-induced pathologic bone remodeling.

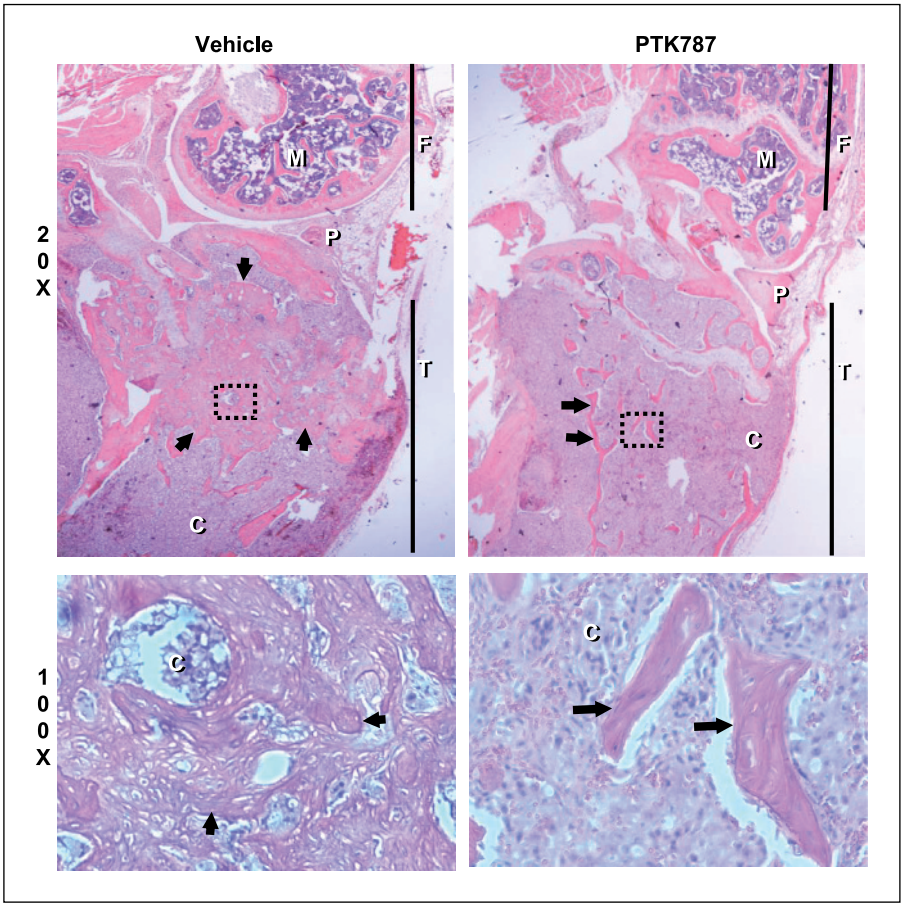

Figure 7. VEGF contributes to C4-2B-mediated induction of osteosclerosis. SCID mice were injected intratibially with C4-2B cells (10^5 in 25 μL RPMI 1640). After 6 weeks of tumor growth, treatment with either PTK787 (n = 12) or distilled water vehicle (n = 9) was initiated and continued for 4 weeks at which time mice were euthanized and bones were subjected to histopathologic analysis. H&E-stained sagittal sections of legs from the distal femur (*F*) through the proximal tibia (*T*); the patella (*P*) is indicated. Note the normal marrow (*M*) cells in the distal femur in contrast to the prostate carcinoma (*C*) cells in the tibia. Magnifications, ×20 (*top*) and ×100 (*bottom*; *dotted square* on *top*). *Arrows,* trabecular bone in the PTK787-treated animals. Compare this with the increased bone area that replaces normal trabeculae in the proximal tibia of the vehicle-treated animal (*arrowheads*). *Boxed area,* 100× magnified region.

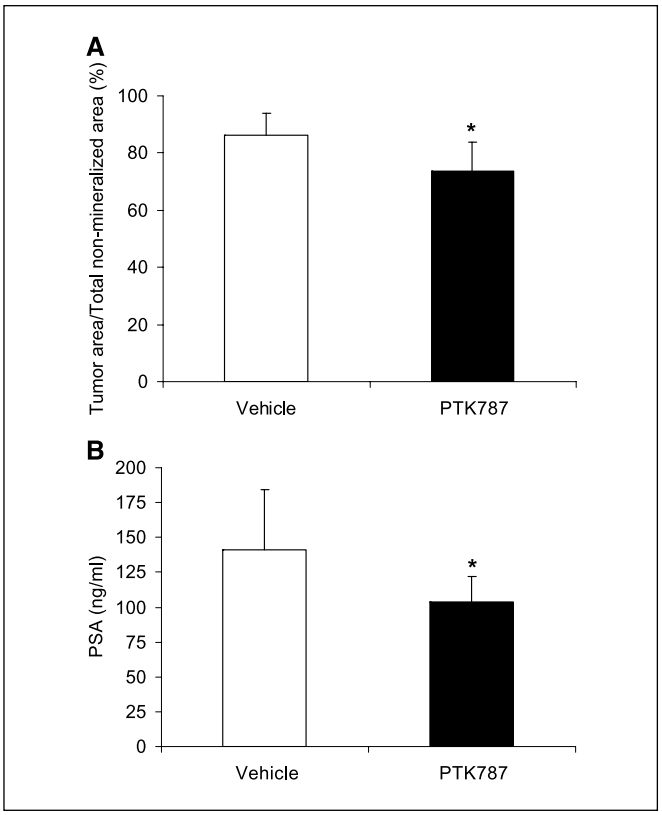

Figure 8. Inhibition of VEGF reduces tumor intratibial C4-2B tumor burden. SCID mice were injected intratibially with C4-2B cells (10^5 in 25 μL RPMI 1640). After 6 weeks of tumor growth, treatment with either PTK787 ($n = 12$) or distilled water vehicle ($n = 9$) was initiated and continued for 4 weeks at which time mice were euthanized, blood was collected and centrifuged to obtain serum, and bones were collected and processed for histology. *A,* tumor area as percentage of total nonmineralized area within the tibia was determined using BioQuant imaging system. *B,* serum was subjected to ELISA for PSA. *, $P < 0.01$ versus vehicle (Student's *t* test).

Discussion

The mechanisms through which prostate cancer induces osteoblastic lesions are currently unknown. In the present study, because of the recently recognized ability of VEGF to induce osteoblast activity, we sought to determine if VEGF contributes to the ability of prostate cancer to induce osteoblastic lesions. Our results showed that C4-2B cells induce osteoblastic differentiation of pre-osteoblastic cells through VEGF. Furthermore, the *in vivo* studies show that VEGF contributes to the development of osteoblastic prostate cancer lesions in bone. These data suggest that prostate cancer promotes osteoblastic metastases partly through the direct action of VEGF on osteoblasts.

Our finding that prostate cancer cells expressed VEGF is consistent with previous publications in which VEGF expression was identified in prostate cancer cells (31–33). We extended these studies by quantifying VEGF protein levels and found that C4-2B cells express higher levels of VEGF protein than LNCaP and PC-3. This observation, taken together with the previous reports that C4-2B cells are more osteoblastic than LNCaP or PC-3 cells (34, 35), is consistent with the hypothesis that VEGF promotes prostate cancer–mediated osteoblastic activity.

Several publications have shown that conditioned medium from prostate cancer cells induces osteoblastic activity *in vitro* (10, 21, 27). However, these studies did not clearly delineate what factors mediated the osteoblastic effect. In the current study, we identified that C4-2B cells induced osteoblastic activity partly through VEGF. We further confirmed that VEGF could directly induce osteoblastic differentiation. These observations support the hypothesis that VEGF plays an important role in the osteoblastic differentiation mediated by prostate cancer. However, the observation that a higher concentration of rhVEGF than that measured in C4-2B conditioned medium was needed to induce alkaline phosphatase and osteocalcin levels and could not induce mineralization of MC3T3-E1 cells indicates that VEGF alone is not sufficient to promote full osteoblastic differentiation. The most likely reason we saw this different effect between prostate cancer conditioned medium and rhVEGF is that prostate cancer cells produce other factors, in addition to VEGF, that may contribute to osteoblastic activity. Osteoblastic factors produced by prostate cancer cells include BMPs, endothelin-1, Wnts, and urokinase plasminogen activator (36, 37). Thus, it is possible that VEGF acts in concert with these factors. Regardless of the other osteoblastic factors present, the observation that PTK787 inhibited C4-2B conditioned medium–induced osteoblastic activity shows that VEGF contributes to the osteoblastic activity of prostate cancer.

In addition to the *in vitro* evidence that VEGF contributes to prostate cancer–mediated osteoblastic activity, our *in vivo* findings provide further support for this concept. The observations that C4-2B induced increased BMD and increased disorganized bone formation within the tibia indicate that this tumor has an osteoblastic component. This was additionally supported by the observation of increased osteocalcin serum levels, which indicates an increase of osteoblastic activity. The observation that PTK787 blocked C4-2B-mediated osteoblastic activity, including both increased BMD and serum osteocalcin, confirmed that VEGF

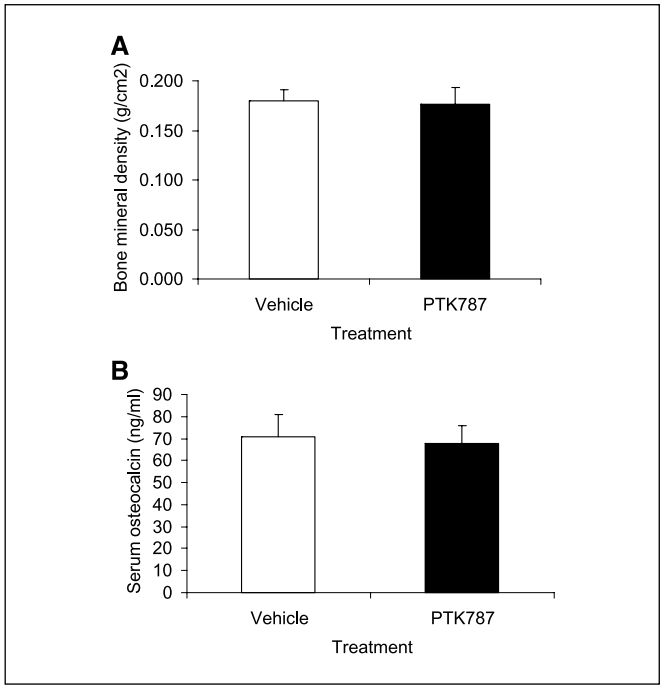

Figure 9. Short-term inhibition of VEGF does not affect bone remodeling of normal bone in mice. Either vehicle or PTK787 was given to mice daily for 4 weeks. Mice were euthanized and serum and tibiae were collected. *A,* tibiae were subjected to DEXA for measurement of BMD. *B,* serum was subjected to osteocalcin enzyme immunoassay.

contributes to the osteoblastic component of C4-2B bone lesions. However, although these data show an important role for VEGF in the development of these osteoblastic lesions, we cannot conclude that this was due totally to decreasing the osteoblastic activity of the prostate cancer cells. Specifically, in addition to decreasing the C4-2B-induced osteoblastic changes in the bone, PTK787 diminished the tumor growth in the bone too (discussed in detail below). Thus, it is possible that the decreased osteoblastic changes were due partly to the fact that there was less tumor burden present in addition to a decreased osteoblastic activity of the tumor itself. The observation that tumor cells were surrounded by new bone in the vehicle-treated animals, whereas tumor cells were not surrounded by bone in the PTK787-treated animals (Fig. 7) provides evidence that the osteoblastic activity of the prostate cancer cells was blocked. This observation, taken together with the *in vitro* data showing that VEGF directly induced osteoblastic activity, suggests that, in addition to decreasing tumor growth, inhibition of VEGF decreases the osteoblastic activity of the prostate cancer cells.

VEGF plays an important role in tumor establishment and progression. In the current study, PTK787 reduced tumor area in the tibia and decreased PSA levels, indicating that inhibition of VEGF diminished growth of prostate cancer in the bone. These results are consistent with previous studies that have shown that inhibition of VEGF using antibodies, kinase inhibitors, or soluble decoy receptors diminished establishment of prostate cancer tumors (38) and progression of established tumors (39–41) in soft tissue sites. However, the degree of intratibial tumor growth inhibition we observed was small (between 15% and 20% based on tumor area measurement and PSA levels) compared with that observed at soft tissues sites in the previous reports (between 60% and 80%). Organ-specific differences may account for the discrepancy in tumor reduction. For example, overexpression of VEGF in C4-2 cells (a precursor to C4-2B cells) increased their growth rate in s.c. sites but not in the bone (42), which indicates that VEGF expression promotes prostate cancer growth in a tissue-specific fashion. The mechanism of how inhibition of VEGF diminished intratibial tumor growth is not known. However, diminished angiogenesis could account for part of this activity, although it has been shown that VEGF expression does not directly correlate with angiogenesis in prostate cancer tumors (43). An alternative explanation is based on the observation that VEGF promotes the ability of prostate cancer cells to migrate (44, 45). Thus, blocking VEGF may have reduced the ability of C4-2B cells to progress in the bone by blocking its ability to migrate within the marrow cavity.

It is not clear what the roles of the different VEGFRs are in pre-osteoblast cells. In the current study, we detected mRNA expression of neuropilin-1 but not Flt-1 or KDR in human osteoblast cells and prostate cancer cells, whereas in MC3T3-E1 cells Flt-1 and neuropilin-1 but not KDR were detected. That VEGF induced the proliferation of HDMECs that expressed KDR but did not affect proliferation of prostate cancer and MC3T3-E1 cells, both that do not express KDR, suggests that KDR mediates the proliferative effects of VEGF. The roles of Flt-1 and neuropilin-1 remain unclear; however, our results indicate the possibility that VEGF promotes osteoblastic differentiation through VEGF signaling pathway using Flt-1 and/or neuropilin-1. PTK787 is primarily considered to inhibit KDR; however, the IC_{50} of PTK787 on Flt-1 is very close to that on KDR (0.077 and 0.037 μmol/L, respectively; ref. 23). Thus, PTK787 would likely inhibit the Flt-1 receptor in this murine model. PTK787 can also inhibit the platelet-derived growth factor-β (PDGF-β) receptor but at between 7- and 20-fold higher IC_{50} than for the VEGFRs (23). Thus, we cannot rule out that some effects we observed were due to inhibition of PDGF-β.

In summary, our data, along with previously published data, suggest the following model. Prostate cancer cells produce VEGF that facilitates the growth of the tumor presumably through enhancing angiogenesis and perhaps migratory ability. As the tumor enlarges, it continues to produce VEGF that binds neuropilin-1 on pre-osteoblasts and induces osteoblast differentiation, in concert with other prostate cancer–produced osteoblastic factors, which result in the development of osteosclerotic lesions. This model indicates that VEGF is an important factor in the development of prostate cancer–induced osteoblastic lesions and thus suggests that targeting the VEGF signaling pathway may provide clinical utility for the prevention and treatment of osteoblastic prostate cancer metastases. One problem with targeting only the osteoblastic activity of prostate cancer would be the unopposed osteoclastic activity that may occur (46). Accordingly, it may be prudent to make the bone microenvironment unsuitable for prostate cancer growth by targeting both prostate cancer–induced osteoblastic and osteoclastic activity. The overall inhibition of prostate cancer–induced bone remodeling provides promise for inhibiting progression of prostate cancer bone metastases.

Addendum

We have recently identified that Wnt and BMP-6 mediate osteoblastic effects of prostate cancer (47, 48).

Acknowledgments

Received 5/26/2005; revised 8/30/2005; accepted 9/19/2005.

Grant support: National Cancer Institute grants R01 CA103109 and P01 CA093900.

The costs of publication of this article were defrayed in part by the payment of page charges. This article must therefore be hereby marked *advertisement* in accordance with 18 U.S.C. Section 1734 solely to indicate this fact.

We thank Novartis for supplying PTK787.

References

1. Greenlee RT, Hill-Harmon MB, Murray T, Thun M. Cancer statistics, 2001. CA Cancer J Clin 2001;51:15–36.
2. Shah RB, Mehra R, Chinnaiyan AM, et al. Androgen-independent prostate cancer is a heterogeneous group of diseases: lessons from a rapid autopsy program. Cancer Res 2004;64:9209–16.
3. Charhon SA, Chapuy MC, Delvin EE, Valentin-Opran A, Edouard CM, Meunier PJ. Histomorphometric analysis of sclerotic bone metastases from prostatic carcinoma special reference to osteomalacia. Cancer 1983;51:918–24.
4. Turner CH. Functional determinants of bone structure: beyond Wolff's law of bone transformation. Bone 1992;13:403–9.
5. Boyce BF, Yoneda T, Guise TA. Factors regulating the growth of metastatic cancer in bone. Endocr Relat Cancer 1999;6:333–47.
6. Deftos LJ. Prostate carcinoma: production of bioactive factors. Cancer 2000;88:3002–8.
7. Yoneda T. Cellular and molecular mechanisms of breast and prostate cancer metastasis to bone. Eur J Cancer 1998;34:240–5.
8. Autzen P, Robson CN, Bjartell A, et al. Bone morphogenetic protein 6 in skeletal metastases from prostate cancer and other common human malignancies. Br J Cancer 1998;78:1219–23.
9. Harris SE, Harris MA, Mahy P, Wozney J, Feng JQ, Mundy GR. Expression of bone morphogenetic protein messenger RNAs by normal rat and human prostate and prostate cancer cells. Prostate 1994;24:204–11.
10. Hullinger TG, Taichman RS, Linseman DA, Somerman MJ. Secretory products from PC-3 and MCF-7 tumor cell lines upregulate osteopontin in MC3T3-E1 cells. J Cell Biochem 2000;78:607–16.
11. Nelson JB, Hedican SP, George DJ, et al. Identification of endothelin-1 in the pathophysiology of metastatic adenocarcinoma of the prostate. Nat Med 1995;1:944–9.

12. Chen HL, Demiralp B, Schneider A, et al. Parathyroid hormone and parathyroid hormone-related protein exert both pro- and anti-apoptotic effects in mesenchymal cells. J Biol Chem 2002;277:19374–81.

13. Cornish J, Callon KE, Lin C, Xiao C, Moseley JM, Reid IR. Stimulation of osteoblast proliferation by C-terminal fragments of parathyroid hormone-related protein. J Bone Miner Res 1999;14:915–22.

14. Ferrara N, Gerber HP, LeCouter J. The biology of VEGF and its receptors. Nat Med 2003;9:669–76.

15. de Vries C, Escobedo JA, Ueno H, Houck K, Ferrara N, Williams LT. The fms-like tyrosine kinase, a receptor for vascular endothelial growth factor. Science 1992;255: 989–91.

16. Terman BI, Dougher-Vermazen M, Carrion ME, et al. Identification of the KDR tyrosine kinase as a receptor for vascular endothelial cell growth factor. Biochem Biophys Res Commun 1992;187:1579–86.

17. Soker S, Takashima S, Miao HQ, Neufeld G, Klagsbrun M. Neuropilin-1 is expressed by endothelial and tumor cells as an isoform-specific receptor for vascular endothelial growth factor. Cell 1998;92:735–45.

18. Mayr-Wohlfart U, Waltenberger J, Hausser H, et al. Vascular endothelial growth factor stimulates chemotactic migration of primary human osteoblasts. Bone 2002;30:472–7.

19. Midy V, Plouet J. Vasculotropin/vascular endothelial growth factor induces differentiation in cultured osteoblasts. Biochem Biophys Res Commun 1994;199:380–6.

20. Street J, Bao M, deGuzman L, et al. Vascular endothelial growth factor stimulates bone repair by promoting angiogenesis and bone turnover. Proc Natl Acad Sci U S A 2002;99:9656–61.

21. Dai J, Kitagawa Y, Zhang J, et al. Vascular endothelial growth factor contributes to the prostate cancer-induced osteoblast differentiation mediated by bone morphogenetic protein. Cancer Res 2004;64:994–9.

22. Turner K, Jones A. Vascular endothelial growth factor in prostate cancer. Urology 2000;56:183.

23. Wood JM, Bold G, Buchdunger E, et al. PTK787/ZK 222584, a novel and potent inhibitor of vascular endothelial growth factor receptor tyrosine kinases, impairs vascular endothelial growth factor-induced responses and tumor growth after oral administration. Cancer Res 2000;60:2178–89.

24. Franceschi RT, Iyer BS. Relationship between collagen synthesis and expression of the osteoblast phenotype in MC3T3-E1 cells. J Bone Miner Res 1992;7: 235–46.

25. Franceschi RT, Iyer BS, Cui Y. Effects of ascorbic acid on collagen matrix formation and osteoblast differentiation in murine MC3T3-E1 cells. J Bone Miner Res 1994; 9:843–54.

26. Siiteri PK, Wilson JD. Testosterone formation and metabolism during male sexual differentiation in the human embryo. J Clin Endocrinol Metab 1974;38: 113–25.

27. Lin DL, Tarnowski CP, Zhang J, et al. Bone metastatic LNCaP-derivative C4-2B prostate cancer cell line mineralizes *in vitro*. Prostate 2001;47:212–21.

28. Zhang J, Dai J, Qi Y, et al. Osteoprotegerin inhibits prostate cancer-induced osteoclastogenesis and prevents prostate tumor growth in the bone. J Clin Invest 2001;107:1235–44.

29. Zhang J, Dai J, Yao Z, Lu Y, Dougall W, Keller ET. Soluble receptor activator of nuclear factor κB Fc diminishes prostate cancer progression in bone. Cancer Res 2003;63:7883–90.

30. Hiltunen MO, Ruuskanen M, Huuskonen J, et al. Adenovirus-mediated VEGF-A gene transfer induces bone formation *in vivo*. FASEB J 2003;17:1147–9.

31. Latil A, Bieche I, Pesche S, et al. VEGF overexpression in clinically localized prostate tumors and neuropilin-1 overexpression in metastatic forms. Int J Cancer 2000;89: 167–71.

32. Strohmeyer D, Strauss F, Rossing C, et al. Expression of bFGF, VEGF and c-met and their correlation with microvessel density and progression in prostate carcinoma. Anticancer Res 2004;24:1797–804.

33. Trojan L, Thomas D, Knoll T, Grobholz R, Alken P, Michel MS. Expression of pro-angiogenic growth factors VEGF, EGF and bFGF and their topographical relation to neovascularisation in prostate cancer. Urol Res 2004;32: 97–103.

34. Wu TT, Sikes RA, Cui Q, et al. Establishing human prostate cancer cell xenografts in bone: induction of osteoblastic reaction by prostate-specific antigen-producing tumors in athymic and SCID/bg mice using LNCaP and lineage-derived metastatic sublines. Int J Cancer 1998;77:887–94.

35. Thalmann GN, Anezinis PE, Chang SM, et al. Androgen-independent cancer progression and bone metastasis in the LNCaP model of human prostate cancer. Cancer Res 1994;54:2577–81.

36. Goltzman D. Mechanisms of the development of osteoblastic metastases. Cancer 1997;80:1581–7.

37. Logothetis CJ, Lin SH. Osteoblasts in prostate cancer metastasis to bone. Nat Rev Cancer 2005;5:21–8.

38. Borgstrom P, Bourdon MA, Hillan KJ, Sriramarao P, Ferrara N. Neutralizing anti-vascular endothelial growth factor antibody completely inhibits angiogenesis and growth of human prostate carcinoma micro tumors *in vivo*. Prostate 1998;35:1–10.

39. Melnyk O, Zimmerman M, Kim KJ, Shuman M. Neutralizing anti-vascular endothelial growth factor antibody inhibits further growth of established prostate cancer and metastases in a pre-clinical model. J Urol 1999;161:960–3.

40. Wedge SR, Ogilvie DJ, Dukes M, et al. ZD6474 inhibits vascular endothelial growth factor signaling, angiogenesis, and tumor growth following oral administration. Cancer Res 2002;62:4645–55.

41. Becker CM, Farnebo FA, Iordanescu I, et al. Gene therapy of prostate cancer with the soluble vascular endothelial growth factor receptor Flk1. Cancer Biol Ther 2002;1:548–53.

42. Krupski T, Harding MA, Herce ME, Gulding KM, Stoler MH, Theodorescu D. The role of vascular endothelial growth factor in the tissue specific *in vivo* growth of prostate cancer cells. Growth Factors 2001;18:287–302.

43. Connolly JM, Rose DP. Angiogenesis in two human prostate cancer cell lines with differing metastatic potential when growing as solid tumors in nude mice. J Urol 1998;160:932–6.

44. Chen J, De S, Brainard J, Byzova TV. Metastatic properties of prostate cancer cells are controlled by VEGF. Cell Commun Adhes 2004;11:1–11.

45. Chevalier S, Defoy I, Lacoste J, et al. Vascular endothelial growth factor and signaling in the prostate: more than angiogenesis. Mol Cell Endocrinol 2002;189: 169–79.

46. Keller ET. The role of osteoclastic activity in prostate cancer skeletal metastases. Drugs Today (Barc) 2002;38: 91–102.

47. Hall CL, Bafico A, Dai J, Aaronson SA, Keller ET. Prostate cancer cells promote osteoblastic bone metastases through Wnts. Cancer Res 2005;65:7554–60.

48. Dai J, Keller J, Zhang J, Lu Y, Yao Z, Keller ET. Bone morphogenetic protein-6 promotes osteoblastic prostate cancer bone metastases through a dual mechanism. 2005;65:8274–85.